Materials Science and Engineering A 371 (2004) 241–250

www.elsevier.com/locate/msea

Using grain boundary engineering to evaluate the diffusion characteristics in ultrafine-grained Al–Mg and Al–Zn alloys

Takashi Fujita [a], Zenji Horita [a], Terence G. Langdon [b,*]

[a] *Department of Materials Science and Engineering, Faculty of Engineering, Kyushu University, Fukuoka 812-8581, Japan*
[b] *Departments of Aerospace & Mechanical Engineering and Materials Science, University of Southern California, Los Angeles, CA 90089-1453, USA*

Received 17 July 2003; received in revised form 2 December 2003

Abstract

Samples of dilute Al–Mg and Al–Zn alloys, containing a minor Sc addition, were processed by equal-channel angular pressing (ECAP) to achieve grain refinement and different distributions of the grain boundary misorientations. Diffusion experiments were conducted on fine-grained alloys with either low or high fractions of grain boundaries having high-angle misorientations and on unpressed coarse-grained samples. The diffusion couples were annealed at temperatures from 493 to 848 K and the interdiffusion coefficients were determined from the concentration profiles using the Boltzmann–Matano technique. The results show the interdiffusion coefficients tend to be higher in fine-grained alloys having high fractions of high-angle boundaries than in fine-grained alloys having high fractions of low-angle boundaries. The experimental data are used to estimate values for the grain boundary diffusion coefficients.

Keywords: Diffusion; Equal-channel angular pressing (ECAP); Grain boundary engineering; Interdiffusion

1. Introduction

Equal-channel angular pressing (ECAP) is a processing technique in which materials are subjected to severe plastic deformation by pressing samples through a die, constrained within a channel, where the channel bends abruptly through an angle that is generally equal to, or very close to, 90° [1,2]. Processing by ECAP has attracted much attention recently because it is now established that it may be used to refine the grain size of metallic alloys to the submicrometer or even the nanometer range [3]. Many reports document the use of ECAP processing to achieve high strength at ambient temperatures [4–6] and superplastic properties at rapid strain rates when testing in tension at elevated temperatures [6–10]. By contrast, there are relatively few descriptions of the use of ECAP in evaluating the diffusion coefficients.

A recent report described diffusion measurements in an ultrafine-grained Al–3 wt.% Mg alloy processed using ECAP [11]. It was shown in these experiments that the fine-grained couples exhibited enhanced diffusivity due to an increasing contribution from grain boundary diffusion and, in addition, this enhancement increased as the annealing temperature was decreased. It was demonstrated also that the experimental results may be used to obtain direct estimates of the grain boundary diffusion coefficients.

The first objective of the present investigation was to extend these earlier measurements to an ultrafine-grained Al–Zn alloy in order to obtain a direct comparison with the results obtained with the Al–Mg alloy. An Al–Zn alloy was selected for this purpose to provide some information on the influence of the atomic size. Thus, the size difference is larger between Al and Mg than between Al and Zn and it is reasonable to anticipate that the size difference may influence the diffusion behavior especially when diffusion takes place along the grain boundaries.

The second objective was based on the recognition that processing by ECAP provides an opportunity not only to examine metallic alloys with exceptionally small grain sizes but also to utilize samples having different distributions of grain boundary misorientation angles so that, as outlined in a recent report [12], ECAP provides a valuable tool for use in grain boundary engineering where materials are utilized

* Corresponding author. Tel.: +1-213-740-0491; fax: +1-213-740-8071.
E-mail address: langdon@usc.edu (T.G. Langdon).

0921-5093/$ – see front matter © 2004 Elsevier B.V. All rights reserved.
doi:10.1016/j.msea.2003.12.042

having different grain boundary character distributions [13]. This approach is based on detailed experimental observations showing that, for pure Al [14] and a wide range of aluminum-based alloys [15], the fraction of high-angle grain boundaries (HAGB) increases with the increasing strain imposed in ECAP.

In practice, the distributions in the boundary misorientations may be significantly changed by selectively rotating the individual samples between each pass in repetitive pressings through an ECAP die. Thus, an array of high-angle boundaries is generally produced most readily when using processing route B_C to large numbers of passes [16] whereas a high fraction of low-angle boundaries is formed when using processing route C to a small number of passes [17,18], where routes B_C and C refer to the procedures of rotating the samples around the longitudinal axes in the same sense by 90° or by 180° between each pass, respectively [19]. Accordingly, the present investigation was designed to compare the effect of the distribution of grain boundary misorientation angles on the diffusion characteristics of Al–Zn and Al–Mg alloys.

It is important to note also that ECAP processing provides a significant advantage over many other processing techniques for the fabrication of ultrafine-grained materials for use in diffusion experiments because grain refinement is achieved in ECAP without the introduction of any residual porosity. Thus, unlike materials processed using conventional powder metallurgy techniques, processing by ECAP leads to ideal materials for diffusion studies because there is an absence of any spurious effects that may arise due to the occurrence of rapid surface diffusion within residual pores.

2. Experimental materials and procedures

Three different alloys, Al–0.1% Sc, Al–3.3% Mg–0.1% Sc and Al–2.1% Zn–0.1% Sc, were prepared through melting and casting processes to dimensions of 20 mm × 60 mm × 120 mm, where all alloy compositions are given in at.%. Scandium was used as an addition in the Al–Mg and Al–Zn alloys because it is known to inhibit significant grain growth during annealing at elevated temperatures [20]. In addition, scandium-reinforced aluminum alloys are currently attracting considerable attention because of their high strength, their beneficial characteristics in welding and their good corrosion resistance [21].

The three cast ingots were homogenized for 86.4 ks (equivalent to 24 h), at temperatures of 873, 753, and 853 K, respectively, and then cut into billets with dimensions of 18 mm × 18 mm × 120 mm. These billets were swaged into rods having diameters of 10 mm and cut to lengths of ∼60 mm for processing by ECAP. Differential scanning calorimetry was used to measure the incipient melting temperatures of the three alloys as 933, 883, and 913 K, respectively. Prior to ECAP, the rods were solution-treated for a period of 3.6 ks (1 h) at temperatures of 903 K for the Al–0.1% Sc alloy, 883 K for the Al–3.3% Mg–0.1% Sc alloy and 913 K for the Al–2.1% Zn–0.1% Sc alloy, where these solution treatment temperatures were selected so that they were essentially at, or very close to, the melting temperatures of each alloy. Following the solution treatments, the average grain sizes were determined as ∼1.2 mm for the Al–0.1% Sc and Al–2.1% Zn–0.1% Sc alloys and ∼0.2 mm for the Al–3.3% Mg–0.1% Sc alloy.

All of the ECAP was performed at room temperature using a solid die having a channel bent through an angle of $\Phi = 90^\circ$ and with an additional angle of $\Psi \approx 20^\circ$ representing the outer arc of curvature at the point of intersection of the two parts of the channel. It can be shown from first principles that these values of Φ and Ψ lead to an imposed strain of ∼1 on each passage of the sample through the die [22]. Repetitive pressings of the same samples were performed up to totals of either 8 passes using route B_C or 2 passes using route C where these two procedures were used to produce arrays of grains having high fractions of either high-angle boundaries or low-angle boundaries, respectively. For each pass through the die, the sample was coated in a lubricant containing MoS_2.

Following ECAP, small blocks with dimensions of 3 mm × 3 mm × 6 mm were cut from each sample for use in the diffusion experiments. On each block, one of the 3 mm × 6 mm planes was mechanically polished followed by electropolishing in a solution of 10% $HClO_4$, 20% $C_3H_8O_3$, and 70% C_2H_5OH. After polishing to a mirror-like finish, two blocks having different compositions were then placed together at their polished surfaces to provide two separate diffusion couples having the following compositions: Al–0.1% Sc/Al–3.3% Mg–0.1% Sc and Al–0.1% Sc/Al–2.1% Zn–0.1% Sc. Prior to coupling, the couple containing the Al–Zn–Sc alloy was immersed quickly in a solution of 40% H_2SO_4 in order to remove any surface oxide layer. Each couple was mounted in an outer window-frame made of stainless steel and then subjected to diffusion annealing at selected temperatures in the range from 493 to 723 K for different periods of time. For comparison purposes, some additional diffusion couples were also prepared from the initial coarse-grained material without using ECAP. All of the diffusion couples were polished on a plane perpendicular to their interfaces for electron probe micro-analysis (EPMA) and the interdiffusion coefficients were determined directly from the concentration profiles using the well-established Boltzmann–Matano method [23,24].

Microstructures were observed before and after diffusion annealing using an Hitachi H-8100 transmission electron microscope (TEM). The orientations of grains within the samples, including the relative fractions of the various grain boundary misorientations, were determined using electron back-scattering diffraction (EBSD) analysis with a JSM-5600 scanning electron microscope equipped with a TSL–EBSD system (OIM-400SPS).

3. Experimental results

3.1. Nature of the microstructures after ECAP and diffusion annealing

Representative as-processed microstructures are shown in Fig. 1 for the Al–2.1% Zn–0.1% Sc alloy after (a) 8 passes through route B_C and (b) 2 passes through route C. These microstructures were taken on the plane perpendicular to the longitudinal axis of the ECAP samples, where this plane is generally designated the *X* plane in investigations of ECAP [18]. Both of these micrographs reveal arrays of ultrafine grains but the larger number of passes, and hence the higher imposed strain, leads to a more equiaxed structure when using route B_C in Fig. 1(a) whereas the grains tend to be elongated in Fig. 1(b) after only 2 passes in route C. After processing using route B_C, the average grain size was measured as ~0.4 μm which is of the same order as the grain sizes of ~0.45 and ~0.27 μm reported earlier for Al–Mg alloys containing 1 and 3 wt.% of Mg [25]. It is apparent from Fig. 1(b) that the grain size was less well-defined after processing with route C and there were many indistinct boundaries and large numbers of intragranular dislocations. Detailed inspection suggested the average grain size in the samples processed using route C was comparable with that attained using route B_C and this conclusion is consistent with extensive earlier measurements on pure Al showing that similar grain sizes are

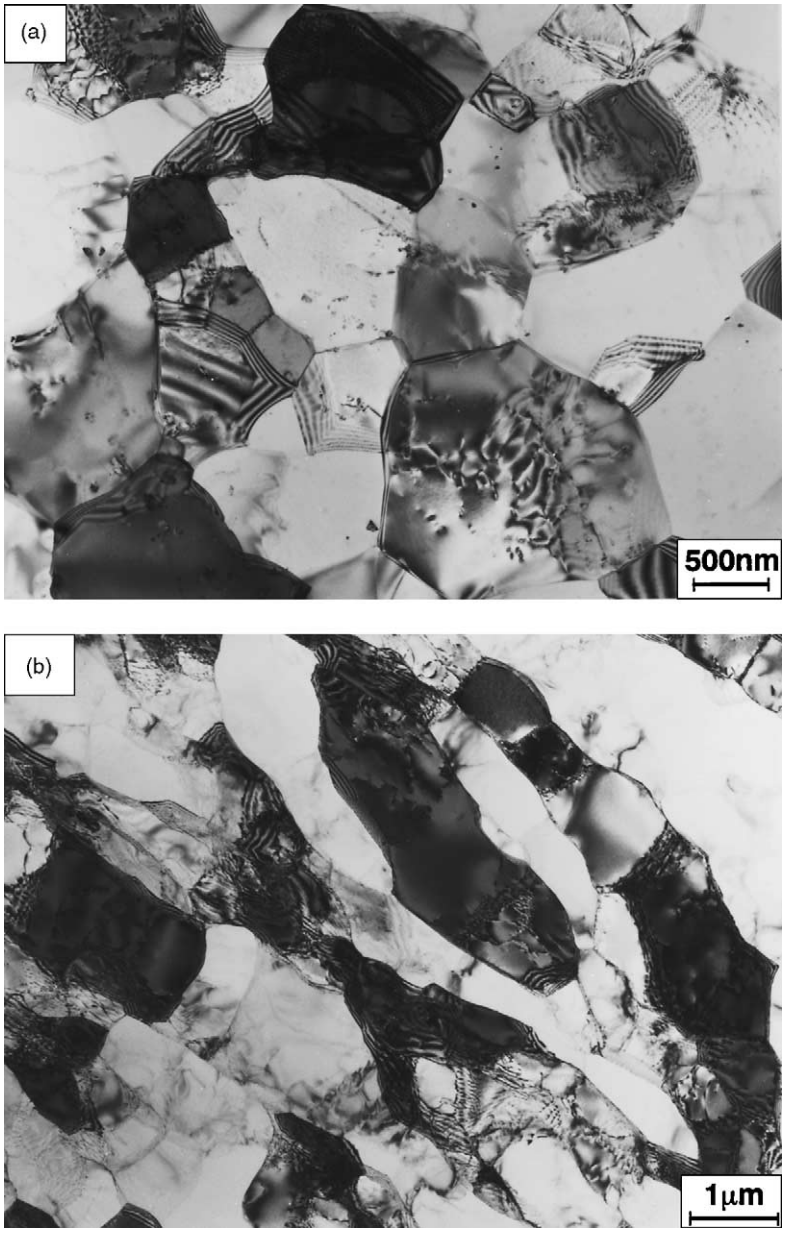

Fig. 1. Microstructures in the Al–2.1% Zn–0.1% Sc alloy after ECAP through (a) 8 passes using route B_C and (b) 2 passes using route C.

achieved when using different processing routes [18]. Essentially similar sets of microstructures were observed also in the Al–0.1% Sc alloy and in the Al–3.3% Mg–0.1% Sc alloy and the average grain sizes of these two alloys were measured after ECAP as ∼0.7 and ∼0.2 μm, respectively.

The EBSD analysis was conducted after processing and diffusion annealing and typical orientation images are shown in Fig. 2 for the Al–2.1% Zn–0.1% Sc samples after (a) 8 passes through route B_C and (b) 2 passes through route C, where both samples were subjected to a diffusion anneal at 523 K for periods of time of (a) 1.73 Ms (20 days) and (b) 432 ks (5 days), respectively. The differences in the microstructures are now more fully revealed by the variations in the color distributions in these two EBSD patterns since each color corresponds to the precise crystallographic orientation of an individual grain as defined in Fig. 2(c). It is apparent that the sample taken through 2 passes using route C in Fig. 2(b) contains grains of fairly similar colors aligned in a banded configuration lying along a preferential direction whereas in Fig. 2(a) the sample taken through 8 passes using route B_C exhibits an essentially random array of equiaxed grains with these various grains displaying wide color variations. In addition, the appearance of these two microstructures shows that the overall extent of grain growth is fairly limited in both samples following the diffusion annealing experiments. Thus, the measured grain sizes were ∼1.2 and ∼1.9 μm for the microstructures in Fig. 2(a) and (b), respectively.

Through a detailed analysis of the EBSD data, the difference in microstructure is revealed in a more quantitative manner in Fig. 3 where the number fractions of each misorientation angle are plotted, in increments of 2.5°, against the measured misorientation angle for the same two samples of the Al–2.1% Zn–0.1% Sc alloy after diffusion annealing following processing by 8 passes in route B_C and 2 passes in route C, respectively: in plotting these histograms, the confidence interval (CI) was set at >0.05 and measurements having a very low reliability were discarded. Defining high-angle boundaries as those having misorientations of ≥15°, it follows from Fig. 3 that there are ∼62% high-angle boundaries and ∼38% low-angle boundaries after processing using route B_C (8 passes) whereas these numbers change to ∼32% high-angle boundaries and ∼68% low-angle boundaries after processing using route C (2 passes). Fig. 4 shows a similar but larger difference in the Al–3.3% Mg–0.1% Sc alloy where the fractions are ∼60% high-angle boundaries and ∼40% low-angle boundaries after processing by route B_C for 8 passes and diffusion annealing for 20 days at 523 K and ∼21% high-angle boundaries and ∼79% low-angle boundaries after processing by route C for 2 passes and diffusion annealing for 5 days at 523 K. All of these measurements reveal very significant variations in the grain boundary misorientation distributions after using these two different processing routes and different imposed strains.

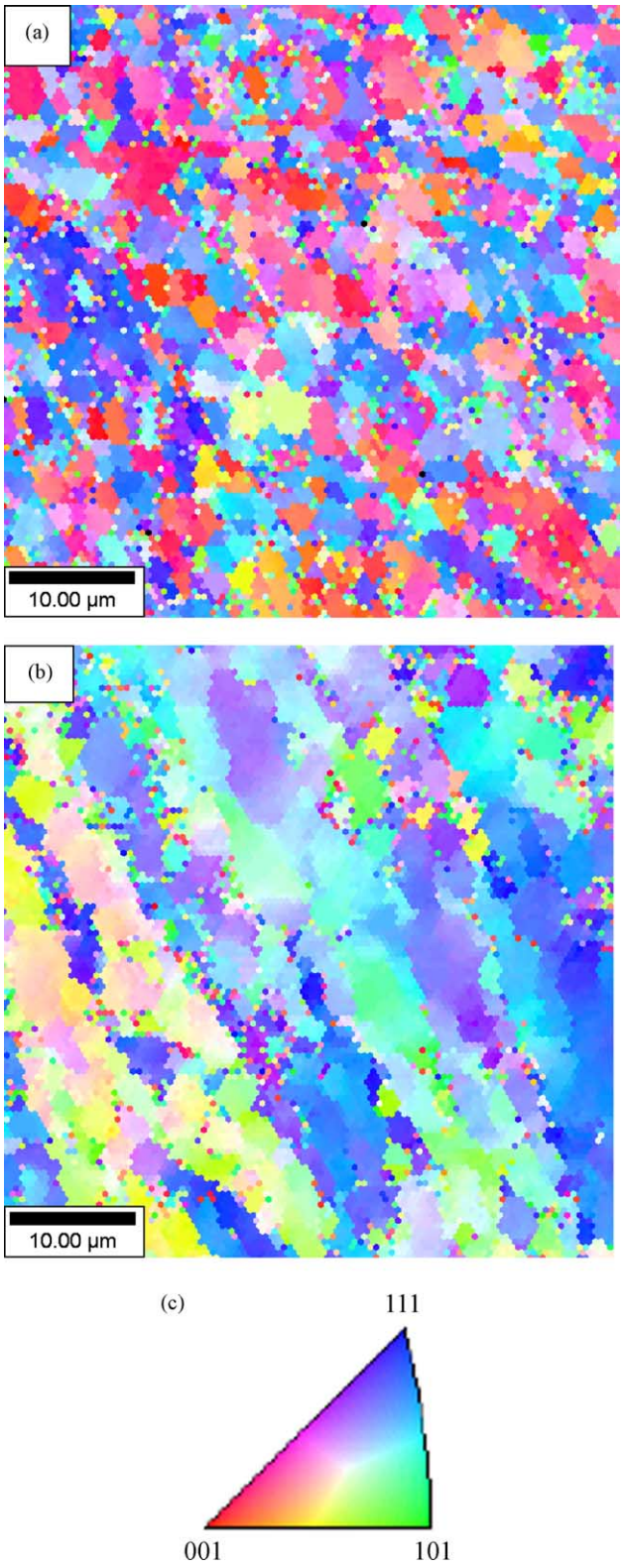

Fig. 2. Orientation images for the Al–2.1% Zn–0.1% Sc specimens after (a) 8 passes through route B_C followed by a diffusion anneal at 523 K for 1.73 Ms (20 days) and (b) 2 passes through route C followed by a diffusion anneal at 523 K for 432 ks (5 days); (c) colors in the crystallographic triangle depict variations in the local orientations.

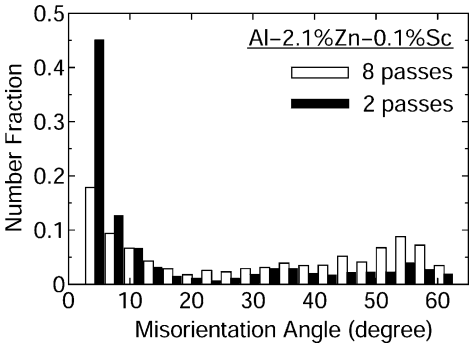

Fig. 3. Distribution of grain boundary misorientations in the Al–2.1% Zn–0.1% Sc alloy for specimens prepared by 8 passes using route B_C or 2 passes using route C; the samples were diffusion annealed at 523 K for either 20 days (route B_C) or 5 days (route C).

3.2. Diffusion measurements

All of the diffusion measurements were conducted on samples prepared by ECAP processing using either route B_C through 8 passes or route C through 2 passes where the microstructures of these two materials are described in detail in the preceding section. It is important to note that the samples processed through route B_C to an imposed strain of ∼8 contained an essentially equiaxed microstructure whereas the samples processed using route C to an imposed strain of ∼2 contained grains that tended to be elongated. It is shown by calculation in Appendix A that the diffusion distances in the present experiments were significantly larger than the average grain sizes so that, accordingly, the minor difference in grain shape was not significant in measurements of the diffusion coefficients.

Fig. 5 shows examples of the concentration profiles measured across the diffusion couple interfaces for (a) the Al–0.1% Sc/Al–3.3% Mg–0.1% Sc diffusion couples and (b) the Al–0.1% Sc/Al–2.1% Zn–0.1% Sc diffusion couples prepared from samples fabricated using three different procedures: ECAP through 8 passes using route B_C to give a fine-grained structure with predominantly high-angle boundaries (designated FG-High), ECAP through 2 passes using route C to give a fine-grained structure with predominantly low-angle boundaries (designated FG-Low) and coarse-grained samples in the solution-treated condition but without ECAP (designated Coarse). The diffusion annealing was undertaken at a temperature of 523 K for each couple and the Matano plane indicated in Fig. 5 denotes the origin of the diffusion distance. The plots show the Mg or Zn concentration, C_{Mg} or C_{Zn}, as a function of the Boltzmann parameter, λ, where λ represents $xt^{-1/2}$ where x and t are the distance from the Matano plane and the total time, respectively. It should be noted that the plots in Fig. 5(a) and (b) specifically employ the time-compensated distance, λ, in order to compensate for the differences in the total time associated with the three couples. In practice, however, the use of $\dot{\lambda}$ in place of x is justified from earlier experiments where it was shown that two distinct concentration profiles, obtained for diffusion couples prepared from samples processed by ECAP after annealing periods differing by a factor of two, may be exactly superimposed by plotting the concentration profiles using λ in place of x [11].

Inspection of Fig. 5 shows that the diffusion distance is longest for the FG-High couple, intermediate for the FG-Low couple and shortest for the unpressed Coarse couple and this same trend is observed in both the Al–0.1%

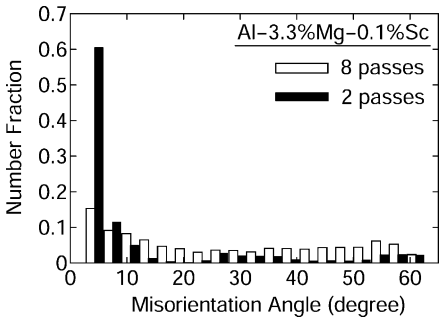

Fig. 4. Distribution of grain boundary misorientations in the Al–3.3% Mg–0.1% Sc alloy for specimens prepared by 8 passes using route B_C or 2 passes using route C; the samples were diffusion annealed at 523 K for either 20 days (route B_C) or 5 days (route C).

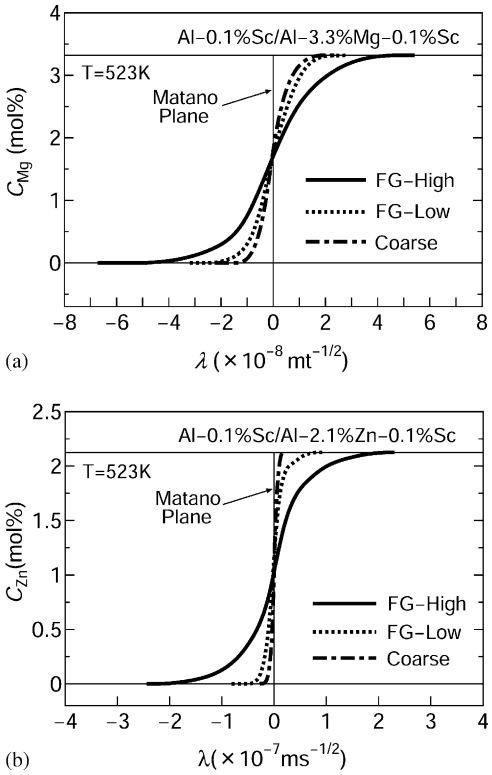

Fig. 5. Concentration profiles of the solute atoms plotted against the Boltzmann parameter, λ, for (a) Al–0.1% Sc/Al–3.3% Mg–0.1% Sc diffusion couples and (b) Al–0.1% Sc/Al–2.1% Zn–0.1% Sc diffusion couples prepared using ECAP through 8 passes with route B_C (FG-High), 2 passes with route C (FG-Low) or coarse-grained samples without ECAP; all couples were annealed at 523 K.

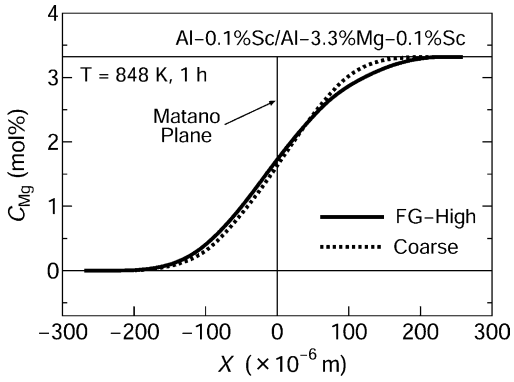

Fig. 6. Profiles of the Mg concentration, C_{Mg}, plotted against the diffusion distance, x, for Al–0.1% Sc/Al–3.3% Mg–0.1% Sc diffusion couples prepared using ECAP through 8 passes with route B_C (FG-High) or coarse-grained samples without ECAP; all couples were annealed at 848 K for 1 h.

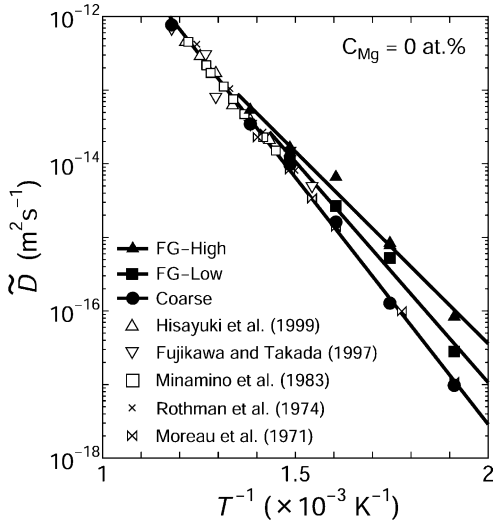

Fig. 7. Arrhenius plots of the impurity diffusion coefficients of Mg in Al obtained from Al–0.1% Sc/Al–3.3% Mg–0.1% Sc diffusion couples prepared using ECAP through 8 passes with route B_C (FG-High), 2 passes with route C (FG-Low) or coarse-grained samples without ECAP; experimental points are included also from published data [26–30].

Sc/Al–3.3% Mg–0.1% Sc and the Al–0.1% Sc/Al–2.1% Zn–0.1% Sc diffusion couples. These results demonstrate, therefore, that the contribution of grain boundary diffusion is significant to the overall diffusion and, furthermore, this contribution becomes more dominant in the FG-High couples than in the FG-Low couples because of the higher fraction of high-angle boundaries.

At higher annealing temperatures, the experiments showed there was no significant difference in the measured diffusion distances. This is demonstrated in Fig. 6 for Al–0.1% Sc/Al–3.3% Mg–0.1% Sc diffusion couples prepared from FG-High and Coarse materials. These two couples were diffusion annealed for 1 h at 848 K and the results are plotted in the form of C_{Mg} versus the uncompensated diffusion distance x. It is important to note that the experimental temperature of 848 K is significantly above the temperature required for the onset of grain growth for both the Al–0.1% Sc and the Al–3.3% Mg–0.1% Sc alloys [20]; the results from earlier static annealing experiments indicate grain sizes of the order of several micrometers in these alloys after annealing for 1 h at 848 K.

Using the Boltzmann–Matano technique, the values of the interdiffusion coefficients, $\tilde{D}$, are plotted against the reciprocal of the absolute temperature, $1/T$, for the Al–0.1% Sc/Al–3.3% Mg–0.1% Sc couples in Fig. 7 and for the Al–0.1% Sc/Al–2.1% Zn–0.1% Sc couples in Fig. 8; in practice, these values correspond to the impurity diffusion coefficients in Al because they were obtained by taking plots of the interdiffusion coefficients determined as a function of C_{Mg} and C_{Zn} and extrapolating to $C_{Mg} = 0$ and $C_{Zn} = 0$. It is apparent from Fig. 7 that the relationship is linear for the Al–Mg system over the entire temperature range covered in these experiments but for the Al–Zn system in Fig. 8 the linearity breaks down for the FG-High couples below ~573 K and for the FG-Low couples below ~523 K. Within the linear portions, the diffusion relationship may be expressed in the conventional form of

$$\tilde{D} = D_0 \exp\left(-\frac{Q}{RT}\right) \quad (1)$$

where D_0 is the preexponential factor; Q, activation energy for diffusion, and R, gas constant. The values estimated for D_0 and Q from these two experimental plots are summarized in Table 1 together with the appropriate error bars for each separate value.

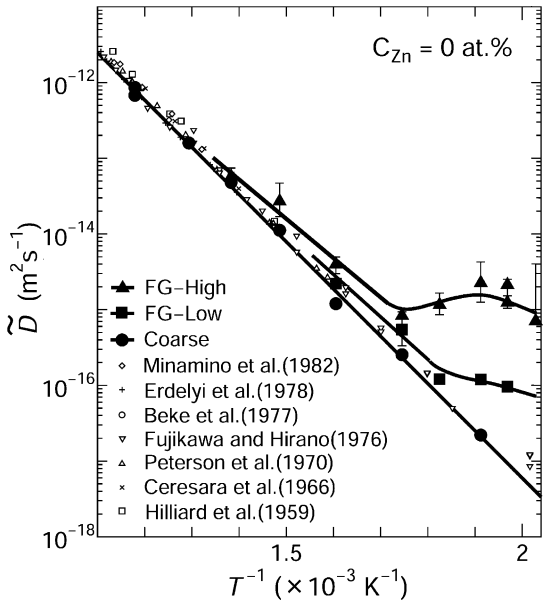

Fig. 8. Arrhenius plots of the impurity diffusion coefficients of Zn in Al obtained from Al–0.1% Sc/Al–2.1% Zn–0.1% Sc diffusion couples prepared using ECAP through 8 passes with route B_C (FG-High), 2 passes with route C (FG-Low) or coarse-grained samples without ECAP; experimental points are included also from published data [31–37].

Figs. 7 and 8 include also numerous datum points obtained from experiments conducted on coarse-grained materials in a series of earlier investigations [26–37]. Inspection shows these additional points lie on, or very close to, the single straight lines determined in this investigation for the coarse-grained specimens in both alloy systems, thereby confirming the general reliability of the present diffusion experiments. It is apparent also that there is a tendency for diffusion to occur most rapidly in the FG-High couples, then in the FG-Low couples and slowest in the coarse-grained couples.

4. Discussion

The experimental results provide a clear demonstration of the potential for using ECAP processing to determine the variation of the diffusion coefficients both with different grain sizes and with different grain boundary character distributions. It is evident from Table 1 that the activation energies associated with the interdiffusion of Mg in aluminum decrease from a high value of $\sim 128 \pm 2\,\mathrm{kJ\,mol^{-1}}$ for the coarse-grained alloy to lower values of $\sim 115 \pm 7\,\mathrm{kJ\,mol^{-1}}$ and $\sim 100 \pm 3\,\mathrm{kJ\,mol^{-1}}$ in fine-grained alloys containing a preponderance of either boundaries with low-angles of misorientation (∼79% of the total distribution) or boundaries with high-angles of misorientation (∼60% of the total distribution). Thus, these results confirm the potential for using ECAP to make changes in the grain boundary character distributions and thus to make use of the general concepts of grain boundary engineering.

A simple procedure may be used to provide a direct estimate of the grain boundary diffusion coefficients for each alloy. As demonstrated earlier [11], the classic relationship for the effective diffusion coefficient introduced by Hart [38] may be manipulated to yield the following relationship:

$$s\delta D_{gb} \approx d\frac{(D_{eff} - D_{lat})}{3} \quad (2)$$

where s is the segregation factor; δ, grain boundary width; D_{gb}, grain boundary diffusion coefficient; d, grain size; and D_{eff} and D_{lat}, effective diffusion coefficient and the lattice diffusion coefficient, respectively. In the present investigation, the values of D_{eff} and D_{lat} correspond to the experimental values measured using the fine-grained couples and the coarse-grained couples, respectively. It was demonstrated also in the earlier investigation [11] that Eq. (2) is consistent with the Monte Carlo simulation developed by Belova and Murch [39].

Table 1
Values of D_0 and Q for interdiffusion of Mg and Zn at $C_{Mg} = 0$ mol% and $C_{Zn} = 0$ mol%

	D_0 ($\mathrm{m^2\,s^{-1}}$)	Q ($\mathrm{kJ\,mol^{-1}}$)
Mg in Al (Coarse)	$(7.5^{+3.7}_{-2.5}) \times 10^{-5}$	128 ± 2
Mg in Al (FG-High)	$(9.9^{+9.1}_{-4.7}) \times 10^{-7}$	100 ± 3
Mg in Al (FG-Low)	$(1.1^{+3.4}_{-0.8}) \times 10^{-5}$	115 ± 7
Zn in Al (Coarse)	$(1.8^{+0.6}_{-0.5}) \times 10^{-5}$	120 ± 2

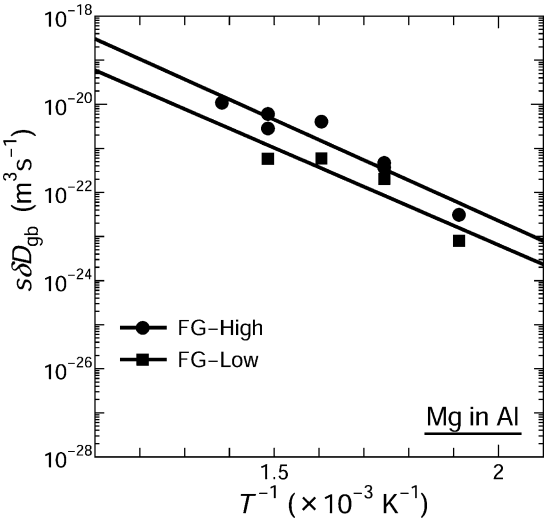

Fig. 9. Arrhenius plots of $s\delta D_{gb}$ for Mg diffusion in Al.

In order to make use of Eq. (2), the values of d were taken as the mean values of the grain sizes measured after diffusion annealing of the fine-grained alloys employed in the diffusion couples. Since it is difficult to obtain reliable values of s and δ for the present alloy systems, the values of the combined term $s\delta D_{gb}$ are plotted in Figs. 9 and 10 for the Al–Mg system and the Al–Zn system, respectively; also included in Fig. 10 are the linear trends reported earlier for diffusion of Zn in Al by Beke et al. [40]. For both alloy systems, it is apparent that the values of $s\delta D_{gb}$ are higher for the alloys containing a preponderance of high-angle boundaries but the individual trends are different. In the Al–Mg system, the individual values fall approximately on two straight lines

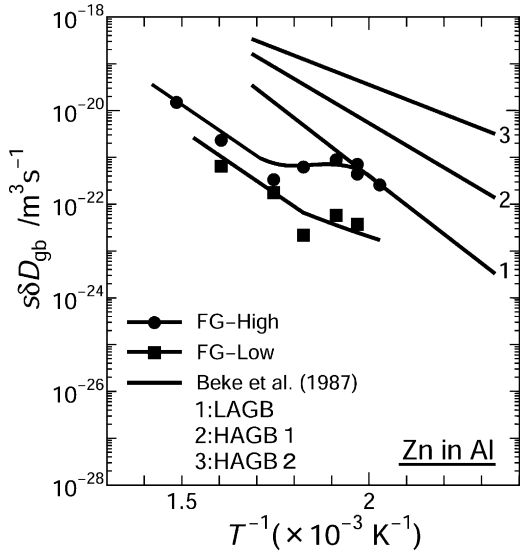

Fig. 10. Arrhenius plots of $s\delta D_{gb}$ for Zn diffusion in Al, including the experimental trends reported by Beke et al. [40].

Table 2
Values of $(s\delta D_{gb})_0$ and Q_{gb} for boundary diffusion of Mg and Zn in Al at $C_{Mg} = 0$ mol% and $C_{Zn} = 0$ mol%

	$(s\delta D_{gb})_0$ ($m^2\,s^{-1}$)	Q_{gb} ($kJ\,mol^{-1}$)
Mg in Al (FG-High)	$(3.4^{+14}_{-2.7}) \times 10^{-14}$	88 ± 8
Mg in Al (FG-Low)	$(4.2^{+236}_{-4.1}) \times 10^{-15}$	84 ± 20
Zn in Al (FG-High) (>573 K)	$(3.9^{+3.8}_{-1.9}) \times 10^{-11}$	122 ± 4
Zn in Al (FG-Low) (>573 K)	$(1.6^{+802}_{-1.6}) \times 10^{-11}$	123 ± 30

having similar slopes within the limited range of temperatures covered in this investigation. By contrast, the Al–Zn system shows only a limited linear region at the higher temperatures above ∼573 K. It is reasonable to conclude that the difference in the diffusion behavior between these two alloy systems is due to the difference in the atomic size of Zn and Mg with respect to the Al matrix.

Defining the preexponential factor and the activation energy for grain boundary diffusion, $D_{0(gb)}$ and Q_{gb}, through the expression

$$D = D_{0(gb)} \exp\left(-\frac{Q_{gb}}{RT}\right) \quad (3)$$

it is possible to use these data to estimate the individual values of $(s\delta D_{gb})_0$ and Q_{gb}. These values are summarized in Table 2 for the two alloy systems shown in Figs. 9 and 10. The value of $Q_{gb} \approx 84$–$88\,kJ\,mol^{-1}$ for grain boundary diffusion of Mg in Al is consistent with the value of $\sim 87\,kJ\,mol^{-1}$ reported earlier [11] and, since Q_{gb} is typically of the order of ∼2/3 of the value for lattice diffusion, it is consistent also with the activation energy of $\sim 130\,kJ\,mol^{-1}$ reported for lattice diffusion of Mg in Al [29] and with the predictions from a molecular dynamics simulation using an embedded atom method [41].

Fig. 10 includes three lines based on the results obtained by Beke et al. [40] where these lines, designated 1, 2, and 3, denote the values obtained for low-angle grain boundaries (LAGB) and high-angle grain boundaries, respectively, with a larger fraction of high-angle boundaries for line 3 than line 2. Inspection of Fig. 10 shows that the measured values of $s\delta D_{gb}$ in the present investigation are a little lower, by about two orders of magnitude, than those reported earlier by Beke et al. [40] but nevertheless the slopes obtained at the higher temperatures are similar to the slope of line 1 for low-angle grain boundaries thereby suggesting that grain boundary diffusion along the low-angle boundaries tends to be dominant at the higher temperatures. As the annealing temperature decreases, however, it is reasonable to anticipate an increasing contribution to the grain boundary diffusion from the presence of high-angle boundaries, thereby giving rise to the experimental deviations from the straight lines. Confirmation of this trend is evident also when it is noted that the deviation occurs at a higher temperature in the couples containing a larger fraction of high-angle grain boundaries: thus, the deviation occurs at a temperature of ∼573 K for the FG-High couples but at a temperature of ∼523 K for the FG-Low couples.

Finally, a direct comparison of Figs. 9 and 10 suggests there is a greater sensitivity to the average grain boundary misorientation in the Al–Zn system than in the Al–Mg system. This difference is probably due to the smaller atomic size of Zn by comparison with Mg. Thus, it is probable that the Mg atoms, having a larger atomic size than Zn, diffuse less easily along the grain boundaries. Furthermore, the results suggest also that this effect may be especially significant at lower temperatures and when the grain boundary misorientation angle is reasonably high.

5. Summary and conclusions

1. Equal-channel angular pressing was used to produce fine-grained Al–0.1% Sc, Al–3.3% Mg–0.1% Sc, and Al–2.1% Zn–0.1% Sc alloys having different fractions of high-angle and low-angle grain boundaries. Diffusion couples were prepared from these fine-grained alloys and the interdiffusion coefficients were measured from the concentration profiles across the interfaces. For comparison purposes, similar measurements were also made using coarse-grained alloys.
2. The results show the measured interdiffusion coefficients tend to be higher in fine-grained alloys having high fractions of high-angle boundaries, intermediate in fine-grained alloys having low fractions of high-angle boundaries and lowest in coarse-grained couples. The values of the grain boundary diffusion coefficients were estimated from the interdiffusion coefficients.
3. The results provide a direct example of the potential for using ECAP processing for the preparation of samples having different grain boundary character distributions for use in evaluating the concepts of grain boundary engineering.

Acknowledgements

We thank Mr. Takayoshi Fujinami for experimental assistance. One of us (T.F.) is grateful to the Japan Society for the Promotion of Science for the award of a Research Fellowship for Young Scientists. This study was supported in part by the Japan Aluminum Association, in part by the Light Metals Educational Foundation of Japan, in part by the US Army Research Office under Grant No. DAAD19-00-1-0488 and in part by the National Science Foundation of the United States under Grant No. DMR-0243331.

Appendix A. An evaluation of the significance of using microstructures with either equiaxed or slightly elongated grains

It is apparent from the microstructures shown in Fig. 1 that the samples prepared by ECAP through 8 passes using

route B_C have essentially equiaxed microstructures whereas the samples prepared by ECAP through 2 passes using route C contain grains that are slightly elongated. This topological difference occurs in addition to the marked variation in the grain boundary characteristics where the samples prepared using route B_C have a high fraction of high-angle grain boundaries and the samples prepared using route C have a high fraction of low-angle boundaries. It is important, therefore, to evaluate whether this difference in grain shape has any significant effect on the results obtained when these two types of samples are used in an analysis of the diffusion behavior.

Harrison [42] classified the diffusion regimes for a system of parallel grain boundaries into three distinct types, termed types A, B, and C, where type A was delineated specifically as the diffusion regime occurring in the limiting situation where the diffusion temperature was high and/or there were very long annealing time and/or the grain size was very small. Under these conditions, the volume diffusion length, defined as $(Dt)^{1/2}$, is significantly larger than the separation between the grain boundaries, defined as the grain size d, where D is the appropriate diffusion coefficient and t is the total time for the diffusion anneal [43]. Thus, type A diffusion requires that

$$(Dt)^{1/2} \gg d \tag{A.1}$$

For the present experiments, considering the Al–0.1% Sc/Al–2.1% Zn–0.1% Sc diffusion couple prepared through route C where the grains tend to be elongated (see Fig. 1(b)), the diffusion anneal was conducted for 5 days so that $t = 4.32 \times 10^5$ s and the effective diffusion coefficient is of the order of $D \approx 10^{-16}\,m^2\,s^{-1}$ so that $(Dt)^{1/2} \approx 6.6\,\mu m$. Thus, the value of $(Dt)^{1/2}$ is significantly larger than the initial grain size of $d \approx 0.4\,\mu m$ measured after ECAP processing and it is also larger, by a factor of more than three times, than the measured grain size of $d \approx 1.9\,\mu m$ following the diffusion anneal. This calculation demonstrates that the condition given by Eq. (A.1) is fulfilled for this experiment and in practice the difference between $(Dt)^{1/2}$ and d is increased even further for the other diffusion conditions. Thus, the present experiments were conducted under conditions appropriate to type A diffusion, primarily because the grain sizes in the samples were exceptionally small, and this leads to the formation of a planar diffusion front [43] such that the results are independent of whether the long axes of any elongated grains are lying parallel or perpendicular to the diffusion couple interface. Under these conditions, the diffusion depth is always proportional to $t^{1/2}$ irrespective of whether points are considered on the grain boundaries or within the interiors of the grains.

In addition, stereographic analysis has shown that the grain boundary area per unit volume, S_v, is related to the mean intercept length between two neighboring grain boundaries, $\bar{L}$, through the simple expression [44]

$$S_v = \frac{2}{\bar{L}} \tag{A.2}$$

Since Eq. (A.2) is valid within any array of grains in a polycrystalline matrix regardless of the average grain shape, it follows that, for materials having similar grain sizes, there is no change in the average grain boundary area, and thus no influence on the diffusivity, even when the grain shape is slightly elongated.

The present analysis confirms conclusively that diffusion occurs in these experiments in the type A diffusion regime and the different topological characteristics are not significant in affecting the nature of the diffusion measurements. On the contrary, the present results lead to measurable differences in the diffusion coefficients for the three sets of samples either processed by route B_C with ultrafine grains, processed by route C with ultrafine grains or not subjected to ECAP with a coarse-grained structure. The results with the coarse-grained microstructure are consistent with earlier published data [26–37] and the differences between the samples prepared using routes B_C and C are due exclusively to the differences in their grain boundary character distributions.

References

[1] R.Z. Valiev, R.K. Islamgaliev, I.V. Alexandrov, Prog. Mater. Sci. 45 (2000) 103.
[2] M. Furukawa, Z. Horita, M. Nemoto, T.G. Langdon, J. Mater. Sci. 36 (2001) 2835.
[3] R.Z. Valiev, N.A. Krasilnikov, N.K. Tsenev, Mater. Sci. Eng. A 137 (1991) 35.
[4] Z. Horita, T. Fujinami, M. Nemoto, T.G. Langdon, Metall. Mater. Trans. 31A (2000) 691.
[5] R.Z. Valiev, I.V. Alexandrov, Y.T. Zhu, T.C. Lowe, J. Mater. Res. 17 (2002) 5.
[6] W.J. Kim, J.K. Kim, T.Y. Park, S.I. Hong, D.I. Kim, Y.S. Kim, J.D. Lee, Metall. Mater. Trans. 33A (2002) 3155.
[7] R.Z. Valiev, D.A. Salimonenko, N.K. Tsenev, P.B. Berbon, T.G. Langdon, Scripta Mater. 37 (1997) 1945.
[8] S. Komura, Z. Horita, M. Furukawa, M. Nemoto, T.G. Langdon, Metall. Mater. Trans. 32A (2001) 707.
[9] K.-T. Park, D.-Y. Hwang, S.-Y. Chang, D.H. Shin, Metall. Mater. Trans. 33A (2002) 2859.
[10] K.-T. Park, D.-Y. Hwang, Y.-K. Lee, Y.-K. Kim, D.H. Shin, Mater. Sci. Eng. A 341 (2003) 273.
[11] T. Fujita, Z. Horita, T.G. Langdon, Phil. Mag. A 82 (2002) 2249.
[12] M. Furukawa, Z. Horita, T.G. Langdon, Interf. Sci. (2003) in press.
[13] T. Watanabe, Res. Mech. 11 (1984) 47.
[14] S.D. Terhune, D.L. Swisher, K. Oh-ishi, Z. Horita, T.G. Langdon, T.R. McNelley, Metall. Mater. Trans. 33A (2002) 2173.
[15] O.V. Mishin, D. Juul Jensen, N. Hansen, Mater. Sci. Eng. A 342 (2003) 320.
[16] K. Oh-ishi, Z. Horita, M. Furukawa, M. Nemoto, T.G. Langdon, Metall. Mater. Trans. 29A (1998) 2011.
[17] Y. Iwahashi, Z. Horita, M. Nemoto, T.G. Langdon, Acta Mater. 45 (1997) 4733.
[18] Y. Iwahashi, Z. Horita, M. Nemoto, T.G. Langdon, Acta Mater. 46 (1998) 3317.
[19] M. Furukawa, Y. Iwahashi, Z. Horita, M. Nemoto, T.G. Langdon, Mater. Sci. Eng. A 257 (1998) 328.
[20] P.B. Berbon, S. Komura, A. Utsunomiya, Z. Horita, M. Furukawa, M. Nemoto, T.G. Langdon, Mater. Trans. JIM 40 (1999) 772.
[21] Z. Ahmad, JOM 55 (2) (2003) 35.

[22] Y. Iwahashi, J. Wang, Z. Horita, M. Nemoto, T.G. Langdon, Scripta Mater. 35 (1996) 143.
[23] L. Boltzmann, Ann. Phys. 53 (1894) 959.
[24] C. Matano, Jpn. J. Phys. 8 (1933) 109.
[25] Y. Iwahashi, Z. Horita, M. Nemoto, T.G. Langdon, Metall. Mater. Trans. 20A (1998) 2503.
[26] K. Hisayuki, T. Yamane, H. Okubo, T. Okada, T. Takahashi, K. Hirao, Z. Metallk. 90 (1999) 423.
[27] S. Fujikawa, Y. Takada, Defect Diffusion Forum 143/147 (1997) 409.
[28] Y. Minamino, T. Yamane, A. Shimomura, M. Shimada, M. Koizumi, N. Ogawa, J. Takahashi, H. Kimura, J. Mater. Sci. 18 (1983) 2679.
[29] S.J. Rothman, N.L. Peterson, L.J. Nowicki, L.C. Robinson, Phys. Stat. Sol. (b) 63 (1974) K29.
[30] G. Moreau, J.A. Corbet, D. Calais, J. Nucl. Mater. 38 (1971) 197.
[31] Y. Minamino, Y. Yamane, M. Koizumi, M. Shimada, N. Ogawa, Z. Metallk. 73 (1982) 124.
[32] G. Erdelyi, D.L. Beke, F.J. Kedves, I. Goedeny, Phil. Mag. B 38 (1978) 445.
[33] D. Beke, I. Goedeny, F.J. Kedves, G. Groma, Acta Metall. 25 (1977) 539.
[34] S. Fujikawa, K. Hirano, Mater. Trans. JIM 17 (1976) 809.
[35] N.L. Peterson, S.J. Rothman, Phys. Rev. B 1 (1970) 3264.
[36] S. Ceresara, T. Federighi, F. Pieragostini, Phys. Stat. Sol. 16 (1966) 439.
[37] J.E. Hilliard, B.L. Averbach, M. Cohen, Acta Metall. 7 (1959) 86.
[38] E.W. Hart, Acta Metall. 5 (1957) 597.
[39] I.V. Belova, G.E. Murch, Defect Diffusion Forum 194–199 (2001) 1223.
[40] D.L. Beke, I. Goedeny, G. Erdelyi, F.J. Kedves, Phil. Mag. A 56 (1987) 659.
[41] C.-L. Liu, S.J. Plimpton, J. Mater. Res. 10 (1995) 1589.
[42] L.G. Harrison, Trans. Faraday Soc. 57 (1961) 1191.
[43] Y. Mishin, C. Herzig, J. Bernardini, W. Gust, Int. Mater. Rev. 42 (1997) 155.
[44] S.A. Saltykov, Stereometric Metallography, second ed., Metallurgizdat, Moscow, 1958, p. 446.